# BOSE-EINSTEIN CONDENSATES OF DILUTE ALKALI VAPOURS: A COHERENT ENSEMBLE OF ATOMS

by W.A. van Wijngaarden and B. Lu

Experiments involving Bose Einstein Condensates of dilute alkali vapours began less than a decade ago. Today, a number of techniques enable condensates to be conveniently studied. An example is given of how to prepare a $^{87}Rb$ condensate in a QUIC trap composed of Quadrupole and Ioffe magnetic field coils. Novel applications of condensates are reviewed including atom interferometry, superfluidity, controlling the speed of light and the behaviour of a coherent array of condensates in an optical lattice. The latter have intriguing implications for quantum computing.

**Novel applications of condensates are reviewed including atom interferometry, superfluidity, controlling the speed of light and the behaviour of a coherent array of condensates in an optical lattice.**

## INTRODUCTION

The importance of spin angular momentum to understanding the structure of matter was realized nearly a century ago. All particles have a spin that is quantized in units of the Planck constant h divided by $2\pi$. Fermions, such as electrons, protons and neutrons have half integral spin while bosons such as photons and mesons have integral spin. Atoms, come in both bosonic and fermionic forms depending on their isotope.

Statistical mechanics shows the average number of particles occupying a state having energy $\varepsilon$ is given by [1]

$$N(\varepsilon) = \{\exp(\varepsilon-\mu) / k_B T \pm 1\}^{-1} \quad (1)$$

where the plus sign applies for fermions and the negative sign for bosons. $k_B$ is Boltzmann's constant, T is the temperature in Kelvins and $\mu$ is the chemical potential which is found by summing the particle populations over all of the energy states to give the total particle number $N_{tot.}$

$$\Sigma_\varepsilon N(\varepsilon) = N_{tot} \quad (2)$$

For fermions at temperatures near absolute zero, equation (1) states that the maximum population of a state is unity. Hence, no two fermions can occupy the same state. For electrons this gives rise to the Pauli Exclusion Principle which is essential for explaining atomic structure. For bosons, there is no limit to the number of particles occupying a given state. Hence, multiple bosons such as photons can be stimulated into the same state to generate a laser beam. All of the particles then have the same properties such as polarization and propagation direction which arise from the constructive interference or coherence of the waves associated with the bosonic particles.

PACS numbers: 03.75, 05.30.Jp, 32.80.Pj, 64.60.-i

The de Broglie wavelength associated with a particle having a mass M is given by

$$\lambda_{dB} = h / (2\pi M k_B T)^{1/2} \quad (3)$$

It increases as the temperature decreases and one intuitively expects the particles to act collectively when the de Broglie wavelength equals the interparticle spacing. Indeed, this is the criterion for Bose Einstein Condensation (BEC) as was first proposed by Bose and Einstein nearly 80 years ago [2,3]. The exact condition for BEC to occur for a 3 dimensional gas in free space is

$$n (\lambda_{dB})^3 > 2.612 \quad (4)$$

where n is the atom density.

It was not until 1938 that F. London realized that superfluid $^4He$ was a BEC [4]. $^4He$ liquefies at a temperature of 4.21 K at atmospheric pressure. It undergoes an additional phase transition at 2.17 K where the specific heat is discontinuous, becoming infinite. This new form of liquid helium exhibits unusual properties including zero viscosity that allows it to pass unimpeded through tiny holes. Hence, it was named a superfluid. Other experiments showed no reduction in the rotation of a superfluid for hours after it was first stirred. Indeed, the circulation given by the integral of the superfluid velocity **v** around a loop was shown to be quantized by Onsager [5] and Feynman [6]

$$\int \mathbf{v} \cdot \mathbf{dl} = n h / M \quad (5)$$

where n is an integer. Hence, the rotation of a superfluid generates tiny whirlpools or vortices each having circulation h/M.

Substitution of the superfluid $^4He$ density of $2 \times 10^{22}$ atoms/cm$^3$ into (4) yields a critical temperature of 3.1 K which exceeds the observed transition temperature. This is not surprising as interparticle interactions have not been considered and these prevent all of the atoms from condensing into the lowest energy state. Indeed, experiments done with helium actually generate a mixture of normal and super fluids. In contrast, studies of alkali atom BECs are done using atom densities of about $10^{13}$ atoms/cm$^3$. Equation (4) then predicts a transition temperature of about 100 nK which is orders of magnitude lower than is attainable using cryogenic

**William Arie van Wijngaarden <wavw@yorku.ca> and Baolong Lu, Department of Physics, York University, 4700 Keele St., Toronto ON M3J 1P3**

techniques. Nearly seven decades of technological progress were required to develop the necessary cooling techniques.

The generation of BEC using alkali atoms requires ultrahigh vacuum to minimize collisions with background gas that would inadvertently cause heating. It is also necessary to trap the atoms to prevent their contacting the vacuum chamber wall. For atoms contained in a trap having a harmonic potential given by

$$V = M (\omega_1^2 x^2 + \omega_2^2 y^2 + \omega_3^2 z^2) / 2 \quad (6)$$

the BEC transition temperature $T_c$ is given by

$$k_B T_c = 0.15 h' \varpi N_t^{1/3} \quad (7)$$

where $h' = h / 2\pi$, $\varpi = (\omega_1 \omega_2 \omega_3)^{1/3}$ and $N_t$ is the number of trapped atoms [7].

There has been an explosion of research in the field of ultracold atoms during the last decade. A number of review articles have been written [8] as well as a comprehensive book by Pethick and Smith [7] discussing ultracold bosons and fermions. The latter were recently used to create molecular BECs [9]. This article focuses on work done with bosons and is organized as follows. First, laser cooling and atom trapping are briefly reviewed. Several types of traps used to attain BEC are discussed next. The case of creating a $^{87}$Rb BEC in a QUIC trap is presented in some detail to illustrate the essential ideas of how to generate and probe a BEC. Finally, a variety of recent applications that illustrate the importance of coherence is reviewed.

## BACKGROUND

### Laser Cooling and Atom Trapping

Cooling samples of atoms to nanoKelvin temperatures has been achieved using laser cooling techniques that are described in the book by Metcalfe and van der Straten [10]. Alkali atoms are ideally suited for this work as they strongly absorb light resonant with their D lines that occur at visible and infrared wavelengths where dye and diode lasers readily operate. They also have relatively low melting points facilitating the production of atomic beams and vapours.

The fundamental basis for laser cooling is that an atom's momentum is reduced when it absorbs an oncoming photon. The excited atom radiatively decays after a short time emitting a photon in no preferred direction. An atom having a mass M and initial velocity v is stopped after absorbing $N_p$ photons given by

$$N_p = M v \lambda / h \quad (8)$$

where $\lambda$ is the resonant laser wavelength. For the case of a $^{87}$Rb atom initially at room temperature, $N_p \approx 50{,}000$. The stopping time, found by multiplying $N_p$ and the 27 nsec lifetime of the Rb $5P_{3/2}$ state is 1.4 ms. During this time, the atom travels a distance of about 20 cm. For an atomic beam consisting of $10^9$ atoms/sec, the laser power required to stop all the atoms is about 10 mW which is readily generated by a diode laser. Once the atom has stopped, it is important that the laser be detuned from resonance to avoid heating the atom. The Doppler cooling limit is given by

$$T_{Dop} = h \Gamma / 2 \quad (9)$$

where $\Gamma$ is the transition linewidth. For the case of $^{87}$Rb, $T_{Dop} \approx 100\ \mu K$. The preceding discussion assumes the slowing atom remains in resonance with the laser beam. In practice, this is accomplished by either tuning or chirping the laser frequency or alternatively by shifting the atomic energies using a magnetic field gradient known as Zeeman tuning.

Cold atoms can be conveniently stored using a magneto-optical trap (MOT) [11]. This consists of a pair of coils whose currents flow in opposite directions such that the magnetic field vanishes at the point midway between the coils. A typical field gradient is about 10 G/cm. Three pairs of counter propagating circularly polarized laser beams traveling in orthogonal directions intersect at the trap center. The so called cooling laser frequency is detuned slightly below resonance as illustrated for $^{87}$Rb in Fig. 1. A second repumper laser depopulates the other ground state hyperfine level for alkali atoms. Whenever an atom wanders from the trap center, the magnetic field shifts it into resonance with an oncoming laser beam. The atom absorbs a photon and is directed back toward the trap center. Atoms can be loaded into a MOT either by slowing an atomic beam or directly from a background atomic vapour. The latter is technically simpler but is not as efficient since the laser is resonant with only a subset of the vapour atoms. Typically, up to $10^9$ atoms can be trapped in a spherical volume having a diameter of less than 1 mm.

The temperature of the trapped atoms is found by suddenly switching the magnetic field off. The laser beams are also

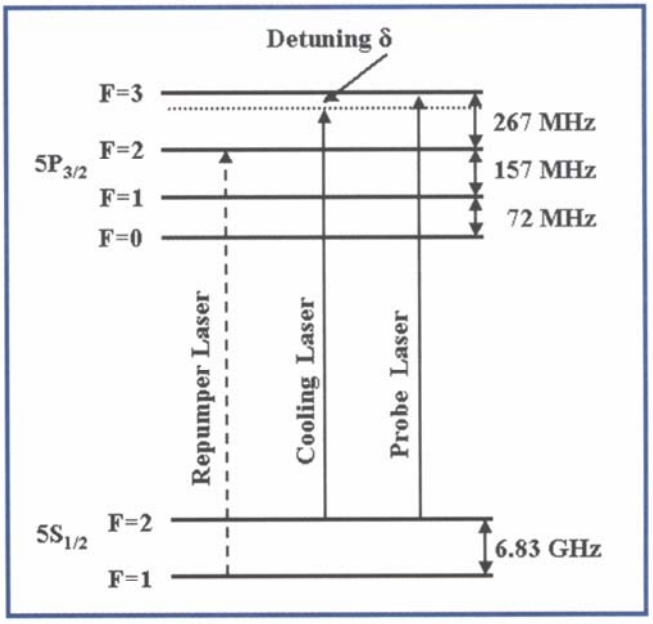


Fig. 1 Relevant $^{87}$Rb Energy Levels and Laser Transitions.

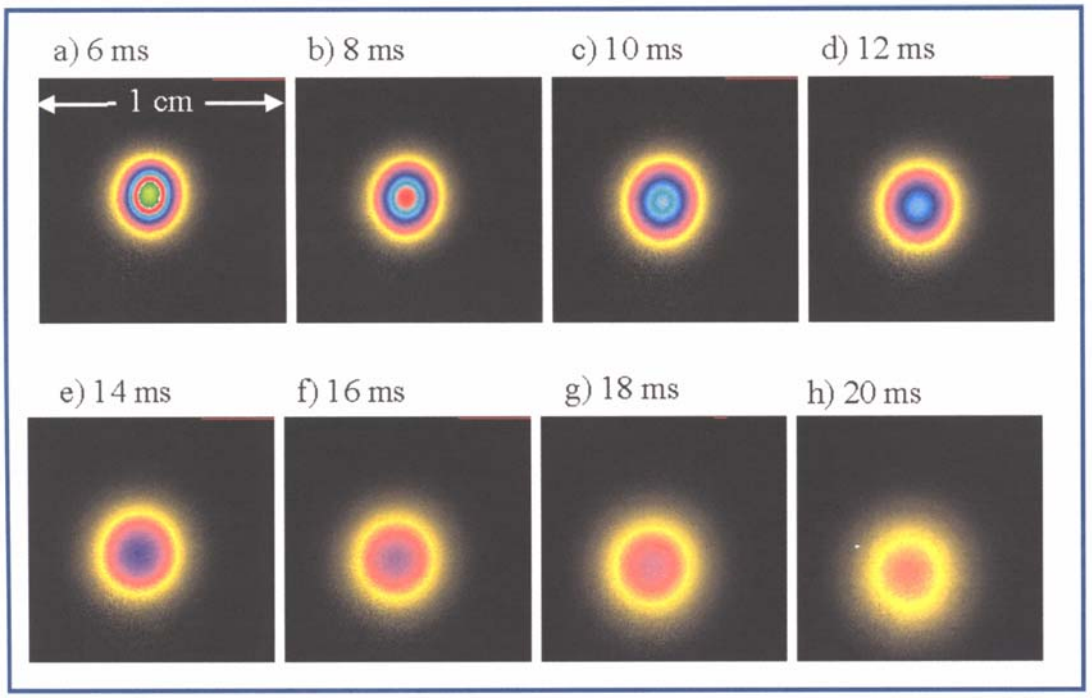


**Fig. 2 Free Expansion of Atom Cloud after Polarization Gradient Cooling for the Times Indicated. Fluorescence was detected using a CCD camera as is described in the text. The atom cloud expanded in time because the atoms have a nonzero temperature and also fell due to gravity.**

blocked and the ultracold atomic cloud is allowed to freely expand. After a certain time, the laser beams are switched back on and fluorescence generated by the atoms is recorded by a CCD camera. The size of the atomic cloud as a function of the free expansion time enables the temperature to be determined. Fig. 2 shows pictures of an expanding $^{87}$Rb cloud taken using various expansion times. The temperature was found to be 50 μK which is below the Doppler cooling limit given by (9). Atoms in a MOT experience a spatially varying laser polarization or gradient generated by the counter propagating laser beams. Detailed analysis shows the atoms preferentially lose energy equal to the light shift when they absorb and reradiate light resulting in cooling below the Doppler limit [12].

### Magnetic Traps

The production of ultracold atoms having suitably low temperature and sufficiently high density to achieve BEC was first done using magnetic traps. This trap consists of two coils having oppositely oriented currents to generate a magnetic field gradient of about 100 G/cm that exerts a force on the atoms balancing gravity and also compresses the cloud increasing the atom density. The magnetic field shifts the energies of the Zeeman sublevels of a hyperfine level. For example, the energies of the $^{87}$Rb $5S_{1/2}$ F = 2 sublevels are given by

$$E(m_F) = g\,\mu_B\,B\,m_F \qquad (10)$$

where $\mu_B$ is the Bohr magneton and g is the Landé factor. Hence, only atoms occupying the $m_F = 1, 2$ sublevels are trapped since their energies are minimized at zero magnetic field. Atoms occupying the other sublevels are expelled from the trap. Optical pumping can transfer atoms into the $m_F = 2$ level before the magnetic trap is turned on.

BEC cannot be attained using only laser cooling techniques as the recoil energy of an atom emitting a single photon corresponds to a temperature that exceeds the BEC threshold temperature. The final stage of cooling is done by applying a radio frequency generated using a small antenna coil located near the trap. This RF frequency causes the atoms to flip their spins from the trapped $m_F = 2$ sublevel to the untrapped sublevels. Initially, this frequency is resonant with atoms far from the trap minimum that experience a larger magnetic field. Hence, hotter atoms are ejected from the trap. The remaining atoms rethermalize as a result of collisions. The RF frequency is tuned slowly to lower frequencies over a time of about half a minute, cooling the atoms to below the BEC transition temperature. This process is called evaporative cooling as it is analogous to a coffee cup cooling as a result of the evaporation of relatively few hot atoms.

A difficulty with magnetic quadrupole traps is that the field vanishes at the trap center and the atoms can therefore undergo Majorana transitions whereby their magnetic dipoles flip and the atom is no longer trapped. A number of creative solutions were developed to "plug this leak". The first experiment to achieve BEC used a so called TOP trap that applied a rotating magnetic field [13]. This shifts the location in the trap where the magnetic field vanishes. The atoms experience a time averaged potential that doesn't vanish anywhere in the trap if the rotating field frequency is on the order of kHz which exceeds typical oscillatory trap frequencies given in (6) which are about $10^2$ Hz. Another approach was to focus an $Ar^+$ laser beam, blue detuned from the Na resonance, at the center of the magnetic trap to repel atoms from this region using the dipole force [14]. Eventually, more elaborate magnetic traps were developed. The MIT group developed the "cloverleaf trap" consisting of a number of coils [15]. A disadvantage of this trap was that several hundred amps were required. It was also necessary

to position the coils in vacuum which posed significant concerns about coil cooling. Another scheme used an arrangement of permanent magnets to create a Li BEC [16]. This has the disadvantage of not being able to vary the magnetic field strength to optimize trap performance. Variations of magnetic traps have been used to Bose condense most of the alkali elements including hydrogen [17] as well as metastable helium [18,19].

A recently developed alternative to the magnetic trap for generating a BEC is the optical trap that uses a pair of counter propagating high power infrared CW laser beams that are focused to a narrow spot [20]. The optical dipole force attracts atoms to the region of high laser intensity if the laser is detuned to the red side of the transition [10]. The laser must be detuned far from resonance in order to avoid resonant transitions that would heat the atoms. Hence, infrared $CO_2$ and Nd:YAG laser beams have been used to create BECs of Rb [20], Cs [21] and Yb [22]. The disadvantage of an optical trap is that it requires an additional laser that generates a power as high as 12 W. However, all magnetic sublevels experience the same trapping force and the optical trap is therefore well suited to trapping atomic states not having a magnetic moment.

### Example of a $^{87}$Rb/ Bose Condensate Using a QUIC Trap

The QUIC trap which was first developed in 1998 [23] consists of a pair of quadrupole coils plus a third so called Ioffe coil that provides a small bias magnetic field at the bottom of the trap as shown in Fig. 3. It requires much smaller currents to generate the necessary trapping magnetic fields compared to other magnetic traps. Furthermore, the coils are located outside the vacuum chamber greatly simplifying the apparatus. Our QUIC trap whose dimensions are illustrated in Fig. 3 generates a magnetic field given by

$$B(y) = B_o + \tfrac{1}{2} K (y - y_{min})^2 \qquad (11)$$

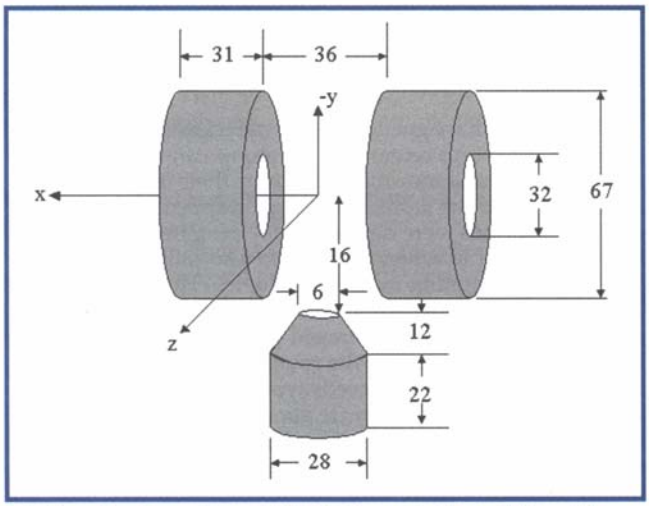


Fig. 3 Configuration of QUIC Magnetic Trap Coils. All dimensions are in mm. The two quadrupole coils each have 181 windings while the lower Ioffe coil has 238 windings of 1.7 mm diameter copper wire.

where $B_o$ = 1.2 G, K = 289 G/cm$^2$ and $y_{min}$ = 7.65 mm [24].

The apparatus to load atoms into the QUIC trap is shown in Fig. 4. $^{87}$Rb atoms were first laser cooled in an upper vapour cell MOT which was maintained at a pressure of about 1 x $10^{-8}$ torr. Atoms were directed into the lower MOT by a pushing laser pulse nearly resonant with the $^{87}Rb\ 5S_{1/2}\ (F= 2) \rightarrow 5P_{3/2}\ (F = 3)$ transition at a rate of 5 Hz for 100 sec. The lower chamber was maintained at a pressure of about 1 x $10^{-11}$ torr by a combination ion titanium sublimation pump. Background pressure was monitored by a residual gas analyzer (RGA) after the system had been baked out. The lifetime of the atoms in the trap exceeded 100 sec allowing sufficient time for evaporative cooling. The BEC was formed at the center of a rectangular quartz cell that had convenient optical access.

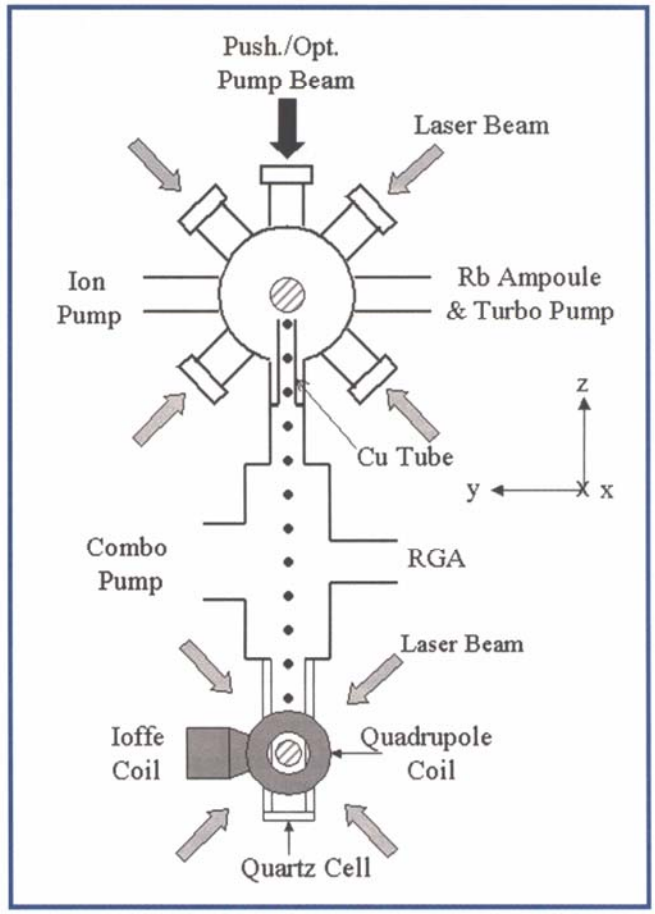


Fig. 4 Vacuum Chamber Layout. The system consists of an upper chamber maintained at a pressure of about 1 x $10^{-8}$ torr using an ion pump and a lower chamber maintained at a pressure of 1 x $10^{-11}$ torr using a combination ion titanium sublimation pump. The pressure is monitored by a residual gas Analyzer (RGA). A 15 cm long copper tube having a diameter of 8 mm is used to maintain the different pressures of the lower and upper chambers.

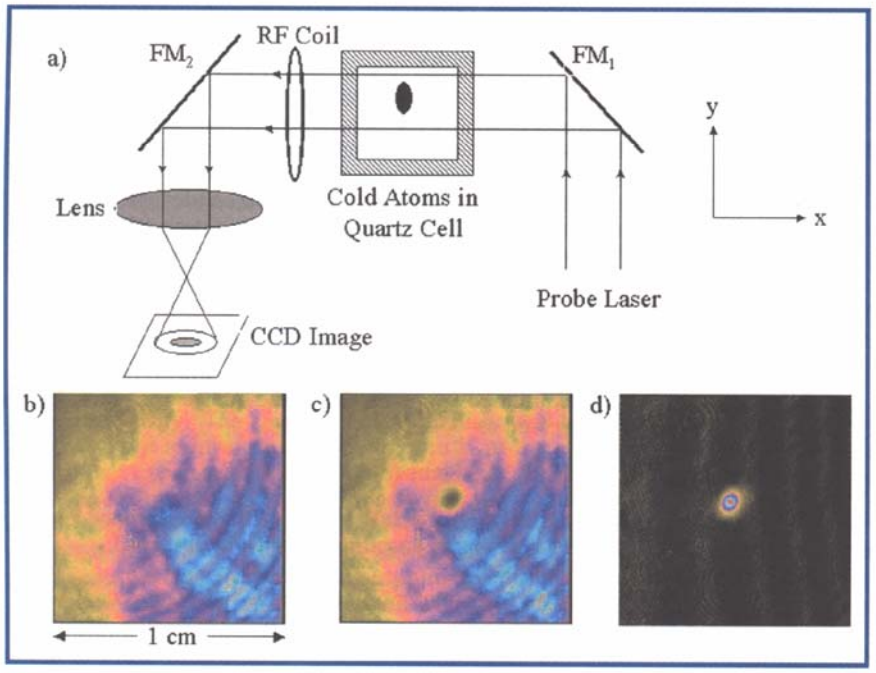


Fig. 5 **Imaging of Cold Atoms using Probe Laser Absorption. The probe laser beam is directed through the ultracold atom cloud using two mirrors $FM_1$ and $FM_2$ that are flipped into position in less than 1 ms. (a) illustrates the apparatus while (b) shows the signal with no atoms in the QUIC trap, (c) shows the signal with $5 \times 10^7$ atoms in the trap. (d) shows the signal produced after the computer processes the data to subtract the background.**

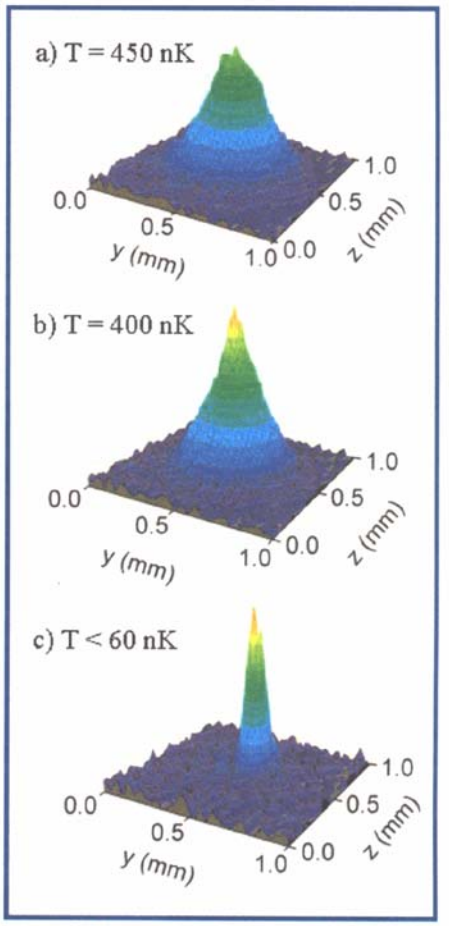


Fig. 6 **Transition to BEC as a Function of Temperature. (a) Thermal Cloud with $N = 1.9 \times 10^6$ atoms at temperature T = 450 nK (b) Mixed thermal atom cloud and BEC where $N = 1.8 \times 10^6$ atoms and T = 400 nK (c) Pure Condensate where $N = 4.2 \times 10^5$ atoms and T < 60 nK.**

Three commercial lasers were used to generate the cooling, repumper and probe laser beams. The laser frequencies were locked using saturation absorption spectroscopy and controlled by acousto-optic modulators. The power, polarization and spatial profile of each laser beam was individually controlled using a myriad of half/quarter waveplates, and spatial filters as described in reference 24. Fibers maintained optical alignment by transporting laser beams from the laser table to the experiment. A computer was interfaced to the various shutters, flipper mirrors and acousto-optic modulators to control the laser pulses with submillisecond timing. Evaporative cooling was accomplished by sweeping the RF from an initial frequency of 20 MHz to a lower frequency over a time of 40 sec.

The ultracold atoms were studied as follows. First, an electronic circuit switched the 25 A magnetic field coil current off in less than 1 ms. The atom cloud was then allowed to freely expand for 24 ms. Finally, a CCD camera monitored the absorption of a 0.1 ms probe laser pulse that was directed through the atom cloud by two mirrors ($FM_1$ & $FM_2$) as illustrated in Fig. 5. The atom number was determined from the optical depth of the atom cloud while the temperature was estimated using the atomic velocity which in turn was found by measuring the distance the atoms traveled during the free expansion time. Temperatures as low as 39 nK were obtained for a sample of about half a million atoms stored in an elliptical region having a volume of approximately 7500 $\mu m^3$.

The transition to BEC is shown in Fig. 6. As the atoms were evaporatively cooled using progressively lower RF final frequencies, a sharp spike emerged in the atom distribution. This is distinct from the Gaussian distribution of thermal atoms. A mixture of thermal atoms and a condensate is obtained at temperatures near the critical temperature. This is illustrated in Fig. 7 which shows the fraction of condensate atoms as a function of the temperature and shows a reasonable fit to the theoretically expected curve.

The time dependent evolution of the condensate is governed by the Gross Pitaevskii equation [7]

$$-h'^2 / 2m \nabla^2 \Psi(r,t) + V(r) \Psi(r,t) + U_o |\Psi(r,t)|^2 \Psi(r,t) = ih' \partial\Psi/\cdot\partial t \qquad (11)$$

which is a modified Schrödinger equation that describes the condensate wavefunction $\Psi$. Hence, $|\Psi|^2$ is proportional to the number of condensate atoms. V is the trap potential and $U_o = ah^2 / \pi M$ results from the van der Waals interaction

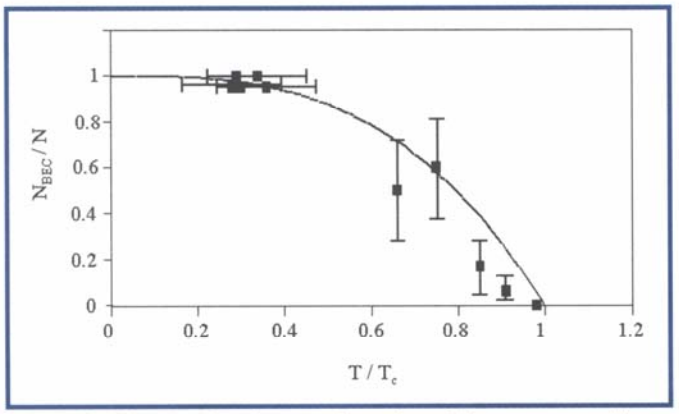


**Fig. 7 Condensate Fraction as a Function of Temperature. The fraction of atoms in the condensate is plotted as a function of the temperature along with the theoretical result $N_{BEC}/N = 1 - (T/T_c)^3$.**

where a is the scattering length for lowest energy or s wave scattering. For $^{87}$Rb, a = 100 Bohr radii. Detailed analysis shows equation (11) predicts the condensate shape oscillates as a function of the free expansion time as shown in Fig. 8 [25]. The scattering length can be precisely determined using photoassociative spectroscopy whereby a laser is tuned to excite an atom of an interacting pair of atoms that then forms a molecular state. The latter can decay generating atoms whose kinetic energies exceed the trap depth resulting in enhanced loss of atoms from the trap [26].

## APPLICATIONS

### Atom Interferometry

The explicit wavelike nature of a BEC has been demonstrated by observing the interference of two condensates [27]. The two condensates were initially spatially separated and each is described by a wavefunction $\Psi(r,t) = f(r,t)\, e^{i\phi(r,t)}$ where $f^2$ is the atom density. The two condensates then freely expanded for a time t overlapping each other. The total condensate wavefunction is given by $\Psi_{tot} = \Psi_1 + \Psi_2$ which has the corresponding atom density.

$$|\Psi_{tot}|^2 = |\Psi_1|^2 + |\Psi_2|^2 + 2\,\mathrm{Re}\,(\Psi_1\Psi_2^*) \qquad (12)$$

For two Gaussian shaped BECs each having an initial width $R_o$ and initial positions $z = \pm d/2$, the interference term can be expressed as [7]

$$2\,\mathrm{Re}\,(\Psi_1\Psi_2^*) \propto \cos\,(h'd\,z\,t\,/\,M\,R_o^2\,R^2) \qquad (13)$$

where $R^2 = R_o^2 + (ht\,/\,2\pi R_o)^2$. Thus, the interference term gives rise to density variations that were observed.

Production of a coherent matter wave has been accomplished using Raman scattering. Two laser beams having slightly different angular frequencies $\omega_1$ and $\omega_2$ and propagation wavevectors $\mathbf{k}_1$ and $\mathbf{k}_2$ are incident on a BEC at rest. Bragg diffraction of the condensate occurs if the energy difference of the photons equals the atom recoil energy

$$h'\,(\omega_1 - \omega_2) = h'^2\,(\mathbf{k}_1 - \mathbf{k}_2)^2\,/\,2M \qquad (14)$$

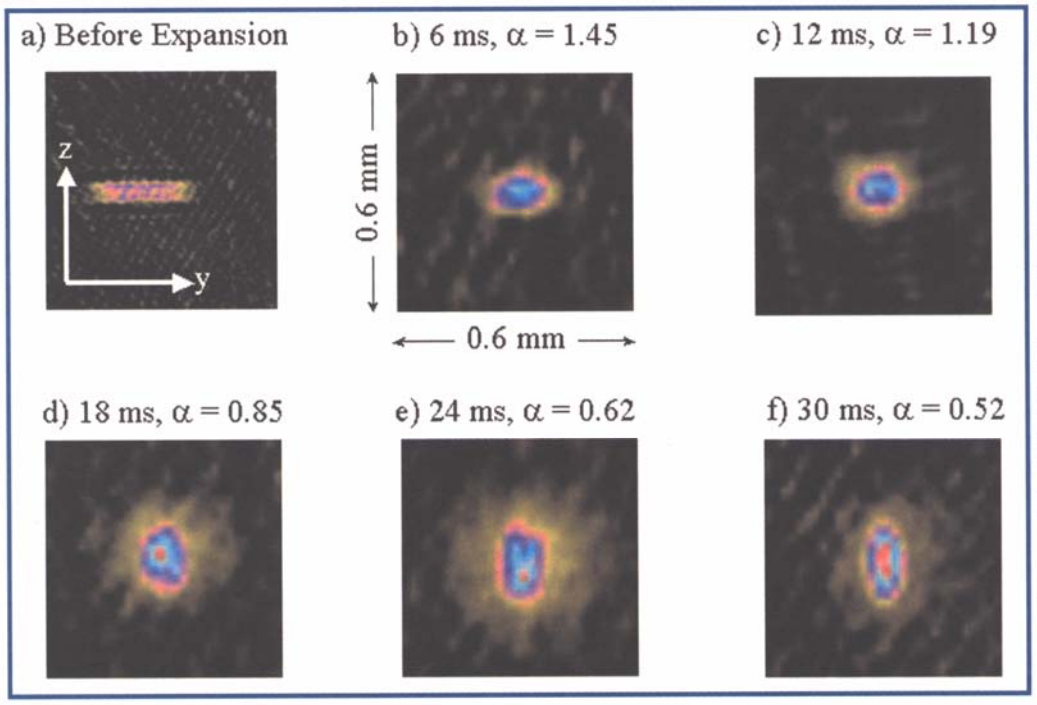


**Fig. 8 Condensate Evolution During Free Expansion for the Times Indicated. α is the ratio of the condensate diameters in the y and z directions. It is a function of the free expansion time. (a) shows the atoms in the trap before the expansion and has a smaller scale than is used in (b) – (f).**

Some of the atoms acquire a velocity $h'(\mathbf{k}_1 - \mathbf{k}_2)\,/\,M$ creating a moving condensate. The MIT group has demonstrated how a moving condensate can be used as a seed matter wave that is input into another condensate and amplified creating a so called atom laser [28]. Of course, a key difference from a conventional photon laser is that the overall number of atoms in the two condensates is conserved. The nonlinear term of equation (11) has also been used to generate soliton pulses of atom waves [29].

### Stopping Light

The very low BEC transition temperature implies that the atoms have low relative velocities and that collisional dephasing is greatly reduced compared to a thermal vapour. Hence, a BEC is

ideally suited for demonstrating electromagnetic induced transparency (EIT). The latter is a quantum interference effect that occurs when a weak probe light field at frequency $\omega_p$ in resonance between atomic states $|1\rangle$ and $|2\rangle$ propagates through a medium with reduced absorption due to the presence of an intense light field that couples states $|2\rangle$ and $|3\rangle$. EIT has been studied using both vapour cells and MOTs and been used to demonstrate optical switching [30]. The coupling laser changes the index of refraction n reducing the speed of light in a condensate to

$$v_g = c\,\{n(\omega_p) + \omega_p\, dn/d\omega_p\}^{-1} \qquad (15)$$

$$\propto I_c\, N^{-1}\, \omega_p^{-1}$$

where $I_c$ is the intensity of the coupling laser beam and N is the atom density. The group of L. Hau first showed how a Na BEC could reduce the speed of light to 17 m/sec [31]. A subsequent experiment actually stopped a light pulse for times up to 1 ms [32]. This was done by first having a short probe laser pulse enter the cold atom cloud that was simultaneously perturbed by a coupling laser beam. The coupling laser was then switched off stopping the probe pulse. The probe pulse was later regenerated when the coupling laser beam reilluminated the atoms.

### Superfluidity

The demonstration of the superfluid properties of a BEC was accomplished by rotating it. This was done using a spatially rotated laser beam to generate a moving potential to perturb the condensate. The condensate velocity is given by

$$\mathbf{v} = h'/M\, \nabla\phi \qquad (16)$$

where $\phi$ is the phase of the condensate wavefunction. Subsequent images of a $^{23}$Na BEC after a free expansion revealed an array of up to 130 vortices each having one unit of quantized circulation h/M as predicted by equation (5) [33].

### Optical Lattices

An array of condensates known as an optical lattice is created by subjecting a BEC to a standing laser wave [34,35]. The atoms are either attracted or repelled from regions of high laser intensity depending on whether the laser is detuned below or above their transition frequency. Optical lattices have been generated in three dimensions using 3 pairs of orthogonal counter propagating laser beams [36]. In practice, the frequencies of the three laser beams are slightly different and none of the laser beams are linearly polarized along the same axis so that the time average of any interference pattern between the orthogonally propagating laser beams is zero. The lattice potential is then given by

$$V = V_o\,\{\sin^2 kx + \sin^2 ky + \sin^2 kz\} \qquad (17)$$

where $k = 2\pi/\lambda$, $\lambda$ is the laser wavelength and $V_o$ is the lattice depth which is proportional to the laser intensity. Here, the laser beams were assumed to have equal intensity which in practice is accomplished using acousto-optical modulators.

At high laser intensity, the atoms are confined to small regions creating a 3 dimensional array of condensates. Condensate atoms can tunnel between neighbouring lattice sites. This is analogous to an electron tunneling between ions in a metal which generates a band structure in the energy spectrum [37]. In the case of the condensate, tunneling of atoms between lattice sites decreases as the laser power increases. This causes a transition from the superfluid state to the so-called Mott insulator state to occur.

The superfluid Mott insulator transition can be modeled using the Bose-Hubbard model which is described by the second quantized Hamiltonian [34].

$$H = -J \Sigma_{ij}\, a_i^t a_j + \Sigma\, \varepsilon_i\, n_i + \tfrac{1}{2}\, U_o\, \Sigma_i\, n_i\,(n_i - 1) \qquad (18)$$

The first term describes tunneling between neighbouring lattice sites i and j. J describes the tunneling probability and $a_i^t$ ($a_i$) is the atom creation (destruction) operator. The second term in (18) is the energy of the atoms at the various lattice sites. $\varepsilon_i$ is the energy of $n_i$ atoms at site i. The last term describes the repulsion between atoms located at the $i^{th}$ lattice site.

In a recent experiment, an optical lattice of $^{87}$Rb atoms was created having over 150,000 lattice sites each containing an average of 2.5 atoms [36]. The coherence was studied by probing the atoms after a free expansion in the usual manner. Superfluid atoms have a fixed relative phase resulting in a structured interference pattern analogous to electron diffraction from a crystal. However, the interference pattern disappeared when the lattice depth exceeded a critical value. Experiment agrees well with theory which predicts a phase transition occurs when $U/J = 5.8\,z$ where z is the number of nearest neighbours of a lattice site [36]. Interestingly, the interference pattern reappeared when the laser intensity was lowered below the transition intensity. The observed time of 14 ms required to restore the coherence is comparable to the tunneling time between neighbouring lattice sites which is proportional to $h'/J$.

## CONCLUSIONS

The field of BEC has developed rapidly in the past decade. In the future, traps with sizes on the orders of microns will undoubtedly play an important role. Microtraps are created using lithographic techniques to deposit carefully configured wires to generate appropriate magnetic fields to trap the atoms [38]. A microtrap has been used to create a BEC in a time of 700 ms which is much faster than is possible using macroscopic traps [39]. Microtraps also require substantially less current and offer tighter atom confinement than conventional traps.

An intriguing possibility is to create an array of microtraps on a chip [40]. Ideally, the microchip would also contain diode lasers not only to interrogate the atoms but also to adjust the coupling between neighbouring condensates by varying the laser power. In practice, such lasers may not have suitably narrow linewidth or stabilized frequency. An alternative would be to direct light generated by a frequency stabilized narrow linewidth laser into fibers that would be embedded in the microchip. This would also simplify the optical alignment.

A microchip array of condensates would be of interest for exploring the possibility of quantum computation [41,42]. The magnetic fields would levitate the atoms above the chip surface reducing the rate of decoherence. Microtrap arrays should be easier to fabricate than competing systems such as the ion trap that requires macroscopic magnetic and electric field electrodes [43]. Controlling coherence in a condensate array will not be simple but progress has been impressive in this field since alkali BECs were first created. In conclusion, BEC studies will certainly remain an exciting research frontier contributing important insights to fundamental physics as well as potentially significant technological applications.

## ACKNOWLEDGEMENTS

The authors wish to gratefully acknowledge the Canadian Natural Science and Engineering Research Council for financial support.

## REFERENCES

1. K. Stowe, *Introduction to Statistical Mechanics and Thermodynamics*, J. Wiley, Toronto, (1984).
2. S.N. Bose, *Z. Phys.*, **26**, 178 (1924).
3. A. Einstein, Sitzungsberichte der Preussischen Akademie der Wissenschaften, Physikalisch-mathematische Klasse (1924).
4. D.R. Tilley and J. Tilley, *Superfluidity and Superconductivity*, Adam Hilger Ltd., Boston, (1986).
5. L. Onsager, *Nuovo Cimento*, **6**, suppl. 2, 249 (1949).
6. R.P. Feynman, *Progress in Low Temperature Physics 1*, ed. C.J. Gorter, (North Holland, Amsterdam, 1955).
7. C.J. Pethick and H. Smith, *Bose-Einstein Condensation in Dilute Gases*, Cambridge Univ. Press, Cambridge, (2002).
8. *Bose Einstein Condensation*, ed. A. Griffin, D.W. Snoke and S. Stringari, Cambridge Univ. Press, Cambridge, (1995).
9. M. Reiner, C.A. Regal and D.S. Jin, *Nature*, **426**, 537 (2003) and C.A. Regal, M. Greiner and D.S. Jin, *Phys. Rev. Lett.*, **92**, 040403, (2004).
10. H.J. Metcalf and P. van der Straten, *Laser Cooling and Trapping*, Springer, New York, (1999).
11. E. Raab, M. Prentiss, A. Cable, S. Chu and D. Pritchard, *Phys. Rev. Lett.*, **59**, 2631 (1987).
12. J. Dalibard and C. Cohen-Tannoudji, *J. Opt. Soc. Am.*, **B6**, 2023 (1989).
13. M.H. Anderson, J.R. Ensher, M.R. Matthews, C.E. Wieman and E.A. Cornell, *Science*, **269**, 198 (1995).
14. K.B. Davis, M.O. Mewes, M. Andrews, M. van Druten, D. Durfee, D. Kurn and W. Ketterle, *Phys. Rev. Lett.*, **75**, 3969 (1995).
15. D. Durfee, PhD Thesis, MIT (1999).
16. C.C. Bradley, C.A. Sackett, J.J. Sackett, J.J. Tollett and R.G. Hulet, *Phys. Rev. Lett.*, **75**, 1687 (1995).
17. D.G. Fried, T.C. Killian, L. Willmann, D. Landhuis, S.D. Moss, D. Kleppner and T.J. Greytak, *Phys. Rev. Lett.*, **81**, 3811 (1998).
18. A. Robert, O. Sirjean, A. Browaeys, J. Poupard, S. Nowak, D. Boiron, C. Westbrook and A. Aspect, *Science*, **292**, 461 (2001).
19. F.P. dos Santos, J. Leonard, J. Wang, C.J. Barrelet, F. Perales, E. Rasel, C.S. Unnikrishnan, M. Leduc and C. Cohen-Tannoudji, *Phys. Rev. Lett.*, **86**, 3459 (2001).
20. M.D. Barrett, J.A. Sauer and M.S. Chapman, *Phys. Rev. Lett.*, **87**, 010401 (2001).
21. T. Weber, J. Herbig, M. Mark, H.C. Nagerl and R. Grimm, *Science*, **299**, 232 (2003).
22. Y. Tahasa, K. Maki, K. Komori, T. Takano, K. Honda, M. Kumakura, T. Yabuzaki and Y. Takahashi, *Phys. Rev. Lett.*, **91**, 040404 (2003).
23. T. Esslinger, I. Bloch and T.W. Hänsch, *Phys. Rev. A*, **58**, R2664 (1998).
24. B. Lu and W.A. van Wijngaarden, *Can. J. Phys.*, **82**, 81 (2004).
25. Y. Castin and R. Dum, *Phys. Rev. Lett.*, **77**, 5315 (1996) and M.O. Mewes, M.R. Andrews, N.J. van Druten, D.M. Kurn, D.S. Durfee and W. Ketterle, *Phys. Rev. Lett.*, **77**, 416 (1996).
26. J. Weiner, V.S. Bagnato, S. Zilio and P.S. Julienne, *Rev. Mod. Phys.*, **71**, 1 (1999).
27. M.R. Andrews, C.G. Townsend, H.J. Miesner, D.S. Durfee, D.M. Kurn and W. Ketterle, *Science*, **275**, 637 (1997).
28. M.O. Mewes, M.R. Andrews, D.M. Kurn, D.S. Durfee, C.G. Townsend and W. Ketterle, *Phys. Rev. Lett.*, **78**, 582 (1997).
29. K.E. Strecker, G.B. Partridge, A.G. Truscott and R.G. Hulet, *Nature*, **417**, 150 (2002).
30. J. Clarke, W.A. van Wijngaarden and H. Chen, *Appl. Opt.*, **40**, 2047 (2000).
31. L.V. Hau, S.E. Harris, Z. Dutton and C.H. Behroozi, *Nature*, **397**, 594 (1999).
32. C. Liu, Z. Dutton, C.H. Behroozi and L.V. Hau, *Nature*, **409**, 490 (2001).
33. J.R. Abo-Shaeer, C. Raman, J.M. Vogels and W. Ketterle, *Science*, **292**, 476 (2001).
34. D. Jaksch, C. Bruder, J.I. Cirac, C.W. Gardiner and P. Zoller, *Phys. Rev. Lett.*, **81**, 3108 (1998).
35. M. Machholm, C.J. Pethick and H. Smith, *Phys. Rev. A*, **67**, 053613 (2003).
36. M. Greiner, O. Mandel, T. Esslinger, T.W. Hänsch and I. Bloch, *Nature*, **415**, 39 (2002).
37. C. Kittel, *Introduction to Solid State Physics*, J. Wiley, Toronto, (1986).
38. M. Dmidic, K.S. Johnson, J.H. Thywissen, M. Prentiss and R.M. Westervelt, *Appl. Phys. Lett.*, **72**, 2906 (1998).
39. W. Hänsel, P. Hommelhoff, T.W. Hänsch and J. Reichel, *Nature*, **413**, 498 (2001).
40. NSERC application proposal by W.A. van Wijngaarden and H. Ruda.
41. J.I. Cirac and P. Zoller, *Phys. Today*, **3**, 38 (2004).
42. O. Mandel, M. Greiner, A. Widera, T. Rom, T.W. Hänsch and I. Bloch, *Nature*, **425**, 937 (2003).
43. D. Leibried, B. DeMarco, V. Meyer, D. Lucas, M. Barrett, J. Britton, W.M. Itano, B. Jelenkovic, C. Langer, T. Rosenband and D.J. Wineland, *Nature*, **422**, 412 (2003).